

Testing interacting dark matter and dark energy model with cosmological data

Gong Cheng,^{1,2} Yin-Zhe Ma,^{3,4} Fengquan Wu,¹ Jiajun Zhang,⁵ and Xuelei Chen^{1,2,6}

¹Key Laboratory of Computational Astrophysics, National Astronomical Observatories,
Chinese Academy of Sciences, 20A Datun Road, Beijing 100101, China

²School of Astronomy and Space Science, University of Chinese Academy of Sciences, Beijing 100049, China

³School of Chemistry and Physics, University of KwaZulu-Natal,
Westville Campus, Private Bag X54001, Durban, South Africa

⁴NAOC-UKZN Computational Astrophysics Center (NUCAC),
University of Kwazulu-Natal, Durban, 4000, South Africa

⁵Center for Theoretical Physics of the Universe,

Institute for Basic Science (IBS), Daejeon, 34126, Korea

⁶Center for High Energy Physics, Peking University, Beijing 100871, China

(Dated: November 13, 2019)

We investigate the model of dark matter-dark energy (DM-DE) interaction with coupling strength proportional to the multiplication of dark sector densities with different power indices $Q = \gamma \rho_c^\alpha \rho_d^\beta$. We first investigate the modification of the cosmic expansion history, and then further develop the formalism to take into account the cosmological perturbations and dark matter temperature evolution. We then use the latest observational cosmology data, including cosmic microwave background (CMB) data, baryon acoustic oscillations (BAO) data, redshift-space distortion (RSD) data and Type Ia supernovae (SNe) data to constrain the model parameters. We find in the phantom region, a positive α is preferred by the data above 2σ statistic significance. If we choose the power indices to be integers or half-integers for *plausible* physics of particle interaction, the allowed values within 1σ confidence regions are $\alpha = 0.5$ and $\beta = 0, 0.5, 1$. The inclusion of BAO and RSD data from large-scale structure and SNe data improves the constraints significantly. Our model predicts lower values of $f(z)\sigma_8(z)$ at $z < 1$ comparing to Λ CDM model, which alleviates the tension of Λ CDM with various RSD data from optical galaxy surveys. Overall, the DM-DE interaction model is consistent with the current observational data, especially providing a better fit to the RSD data.

I. INTRODUCTION

Recently, the *Planck* measurement of the cosmic microwave background radiation (CMB) produces the best-fitting cosmological parameters, which are in good agreement with the low redshift observations (e.g., Baryon Acoustic Oscillation (BAO) from galaxy survey, Type-Ia supernovae data (SNe) and galaxy lensing measurements) [1]. However, there is a roughly 2.5σ confidence level (C.L.) tension between the base *Planck* Λ CDM cosmology prediction and the DES combined-probe results (the later prefers a lower late-time clustering amplitude σ_8 or matter density Ω_m). Besides, the *Planck* base Λ CDM cosmology requires $H_0 = (67.4 \pm 0.5) \text{ km s}^{-1} \text{ Mpc}^{-1}$, which leads to a 4.0σ – 5.8σ tension with the local Hubble constant measurements depending on the approaches used [2]. Many new observations of Hubble constant and new physics trying to explain the discrepancy are discussed in Ref. [2].

Theoretically, new ideas beyond Λ CDM model are developed, aiming to solve the well-known cosmological constant problem and coincidence problem. Moreover, it has been pointed out that the effective field theory that compatible with string theory should satisfy the swampland criteria, while the cosmological constant scenario does not [3].

One possible way to alleviate these problems is to consider the interaction between dark sectors [4]. It is reported that the H_0 and σ_8 tension could be solved or

reduced simultaneously by considering an interaction in the dark sector [5, 6]. Also, it could alleviate the coincidence problem by allowing a constant ratio of dark sector densities [7]. In Ref. [8], the authors explore the possibility that the interaction functions possess a minimum and argue that this model could alleviate the tension between the swampland conjectures and the quintessential potential [8]. Besides, in the framework of field theory, it is natural and inevitable to consider such interactions between dark sectors, and the investigation of the interaction could help us to understand the nature of them [9].

Various models are proposed and tested in the literature (for reviews, see [10–12]). A much studied case is $Q = H(\xi_1 \rho_c + \xi_2 \rho_d)$. Other models are also considered, such as $Q = \Gamma(\dot{\rho}_c + \dot{\rho}_d)$ [13], $Q = H\Gamma\rho_c\rho_d/(\rho_c + \rho_d)$ [14], where ρ_c and ρ_d are the energy densities of dark matter and dark energy respectively and Γ, ξ_1, ξ_2 describe the interaction strength. Besides, the holographic principle is applied in some work [11, 15] and the coupled quintessence model is discussed in Ref. [16].

However, a physically more plausible form of interaction form is for the interaction term to be proportional to the product of the densities of interacting components or some powers of these [15, 17]. For example, in the familiar case of chemical reactions this is the case. Thus a natural way to construct the phenomenological model is to suppose the interaction term is proportional to some

powers of the densities,

$$\dot{\rho}_c + 3aH\rho_c = a\gamma\rho_c^\alpha\rho_d^\beta, \quad (1)$$

$$\dot{\rho}_d + 3a(1+w)H\rho_d = -a\gamma\rho_c^\alpha\rho_d^\beta, \quad (2)$$

where the dot denotes the time derivative with respect to the conformal time and a is the scale factor. In this work, we consider a minimal model in which the equation of state of dark energy w is a constant. The power index α, β are assumed to be non-negative numbers. If we set the indices to be simple integers, the model could reduce to the interactions in the usual sense, such as ‘‘decay’’ (if one is 0 and the other is 1), ‘‘annihilation’’ (if one is 0, and the other is 2). And $\gamma > 0$ indicates dark energy is converted to dark matter, while $\gamma < 0$ indicates the opposite process.

Previous work on the interacting dark energy models mainly focuses on the impact on the background evolutions and expansion history. However, from the theoretical point of view, the inhomogeneity of dark matter will naturally lead to dark energy perturbations as the energy transfers between the two components. And the change of density and velocity perturbations will influence the structure formation and some observational effects (e.g., redshift space distortion). So in this paper, we also investigate the impact on the growth of cosmological perturbations.

Notably, as the perturbed interaction four-vector δQ^ν cannot be determined uniquely by the background interaction form Q , the formalisms developed by different groups differ from each others slightly. In Refs. [18–20], $\delta Q^\nu = \delta Q u_c^\nu/a$ or $\delta Q^\nu = \delta Q u_d^\nu/a$ is assumed to avoid momentum transfer in the rest frame of dark sector, where u_d^ν and u_c^ν are the four velocities. In Refs. [9, 21], on the other hand, the authors assume the energy transfer is stationary and non-gravitational interaction between dark sectors does not exist and so the non-vanishing component is $\delta Q^0 = \delta Q/a$. We regard the later assumption as a more natural choice and follow it to develop the formalisms in our model.

II. FORMALISMS

In this section, we present the formalisms of background evolutions, linear perturbations and thermodynamics in this model. The background evolutions of dark matter and dark energy are described by Eqs. (1) and (2). Due to the energy transfer, the energy-momentum tensor of each component ($\lambda = c, d$) is no longer conserved,

$$\nabla_\mu T_{(\lambda)}^{\mu\nu} = Q_{(\lambda)}^\nu, \quad (3)$$

$$Q = aQ_c^0 = -aQ_d^0 = \gamma\rho_c^\alpha\rho_d^\beta, \quad (4)$$

where Q is the energy transfer rate with respect to the cosmic time and the spatial component $Q_{(\lambda)}^i$ is zero in the background level. For convenience, we use the critical density today to define the dimensionless interaction

parameter as

$$\lambda = \gamma\rho_{\text{cr}}^{\alpha+\beta-1}H_0^{-1}, \quad \rho_{\text{cr}} = 3H_0^2 M_{\text{pl}}^2. \quad (5)$$

For the linear perturbations in the presence of the interaction, we first review the formalisms developed in Refs. [9, 21, 22], and then apply them in this model. Assuming that there is no non-gravitational interaction between dark energy and dark matter, and the energy transfer is stationary, the perturbed four-vector in the synchronous gauge is,

$$\delta Q_c^0 = -\delta Q_d^0 = \frac{1}{a}\delta Q, \quad (6)$$

$$\delta Q_{\text{p}(\lambda)} = Q_{\text{p}(\lambda)}^I \Big|_{\text{t}} + Q_{(\lambda)}^0 v_{\text{t}} = 0. \quad (7)$$

$\delta Q_{\text{p}(\lambda)}$ is the potential of $\delta Q_{(\lambda)}^i$, $Q_{\text{p}(\lambda)}^I \Big|_{\text{t}}$ denotes the external non-gravitational force density between the two components and v_{t} is the energy transfer velocity. Based on this formalism, we obtain the density and velocity perturbation equations for dark matter and dark energy in our model,

$$\dot{\delta}_c = -(\theta_c + \frac{\dot{h}}{2}) + a\gamma\rho_c^{\alpha-1}\rho_d^\beta[(\alpha-1)\delta_c + \beta\delta_d], \quad (8)$$

$$\dot{\theta}_c = -aH\theta_c - a\gamma\rho_c^{\alpha-1}\rho_d^\beta\theta_c + k^2 c_e^2 \delta_c, \quad (9)$$

$$\begin{aligned} \dot{\delta}_d = & -(1+\omega)(\theta_d + \frac{\dot{h}}{2}) + 3aH(\omega - c_e^2)\delta_d \\ & - a\gamma\rho_c^\alpha\rho_d^{\beta-1}[(\beta-1)\delta_d + \alpha\delta_c] - 3aH \\ & (c_e^2 - c_a^2)[3aH(1+\omega) + a\gamma\rho_c^\alpha\rho_d^{\beta-1}]\frac{\theta_d}{k^2}, \end{aligned} \quad (10)$$

$$\begin{aligned} \dot{\theta}_d = & -aH\theta_d(1-3c_e^2) - \frac{\dot{w}}{1+w}\theta_d + \frac{1}{1+w} \\ & (1+c_e^2)a\gamma\rho_c^\alpha\rho_d^{\beta-1}\theta_d + \frac{k^2 c_e^2 \delta_d}{1+w}, \end{aligned} \quad (11)$$

where we have used the form of the perturbed pressure of dark energy in a general frame [9, 23],

$$\delta P_d = c_e^2 \delta_d \rho_d + (c_e^2 - c_a^2) \left[\frac{3aH(1+\omega)\theta_d \rho_d}{k^2} - a^2 Q_d^0 \frac{\theta_d}{k^2} \right]. \quad (12)$$

In practice, we set the effective sound speed of dark energy in the rest frame $c_e = 1$ and adiabatic sound speed of dark energy $c_a^2 = w$.

We set the adiabatic initial conditions for the perturbations following [24]. In order to obtain analytical solutions of initial conditions, we neglect all the interaction terms when solving the continuity and Euler equations.

So our initial conditions are identical with Ref. [24].

$$\delta_c = \frac{3}{4}\delta_\gamma = -\frac{1}{2}C(k\tau)^2, \quad (13)$$

$$\theta_c = 0, \quad (14)$$

$$\theta_\gamma = -\frac{1}{18}C(k^4\tau^3), \quad (15)$$

$$\begin{aligned} \delta_d &= -\frac{C}{2}(1+w)\frac{4-3c_e^2}{4-6w+3c_e^2}(k\tau)^2 \\ &= \frac{1+w}{7-6w}\delta_c, \end{aligned} \quad (16)$$

$$\theta_d = -\frac{C}{2}\frac{c_e^2}{4-6w+3c_e^2}(k\tau)^3k = \frac{9}{7-6w}\theta_\gamma, \quad (17)$$

where γ corresponds to photons and C is a constant.

Besides, the term $k^2c_e^2\delta_c$ appearing in the RHS of $\dot{\theta}_c$ is always ignored by previous work. Nevertheless, compared with Λ CDM model, δ_c and c_c are affected by the interaction. Hence this term might be enhanced and should be taken into account. It's necessary to investigate the contribution of this term to $\dot{\theta}_c$. The sound speed of dark matter c_c is defined as [22]

$$c_c^2 = \frac{k_B T_c}{m_c} \left(1 - \frac{d \ln T_c}{3d \ln a} \right), \quad (18)$$

where m_c is the mass of dark matter particle. We follow the methods in Refs. [25, 26] to calculate the temperature evolution of dark matter in the interacting model using the second law of thermodynamics and obtain

$$\begin{aligned} \dot{T}_c &= \left(\frac{\partial T_c}{\partial n_c} \right)_{\rho_c} \dot{n}_c + \left(\frac{\partial T_c}{\partial \rho_c} \right)_{n_c} \dot{\rho}_c \\ &= \left(\frac{\partial T_c}{\partial n_c} \right)_{\rho_c} \left(-3aHn_c + \frac{aQ}{m_c} \right) \\ &\quad + \left(\frac{\partial T_c}{\partial \rho_c} \right)_{n_c} (-3aH\rho_c + aQ) \\ &= -2aHT_c \left(1 - \frac{\gamma\rho_c^{\alpha-1}\rho_d^\beta}{3H} \right), \end{aligned} \quad (19)$$

where we have used $T \left(\frac{\partial p}{\partial \rho} \right)_n = (\rho+p) \left(\frac{\partial T}{\partial \rho} \right)_n + n \left(\frac{\partial T}{\partial n} \right)_\rho$, $\left(\frac{\partial p_c}{\partial \rho_c} \right)_{n_c} = 2/3$ and n is the number density. As the wrong relation $\left(\frac{\partial p_c}{\partial \rho_c} \right)_{n_c} = w_{\text{eff}} = w_c - \frac{Q}{3H\rho_c}$ is used in Ref. [26], Eq. (34) in Ref. [26] is related to Eq. (19) in this paper by a factor 2/3.

To solve the above equation numerically, we need to set the initial temperature in the early universe. If we assume $T_c = 0$ initially, we obtain a trivial solution, as the macroscopic interaction of the dark matter does not generate the microscopic motion and temperature. Here we set the initial temperature as evolved from earlier time, assuming that dark matter annihilates to baryons through weak-scale interactions at high energies [27],

$$T_c(z) = T_b(z) \quad \text{at} \quad H(z) = \langle \sigma_w v \rangle \rho_c(z)/m_c, \quad (20)$$

TABLE I: BAO measurements from various surveys adopted in this work.

Redshift	Measurement	Value	Surveys
0.106	r_s/D_V	0.327 ± 0.015	6dFGS [34]
0.15	D_V/r_s	4.47 ± 0.16	SDSS DR7-MGS [35]
0.35	D_V/r_s	9.11 ± 0.33	SDSS DR7-LRG [36]
0.38	$D_M(r_{s,\text{fid}}/r_s)$	1518.4 ± 22.4	SDSS DR12-BOSS [37]
0.38	$H(z)(r_s/r_{s,\text{fid}})$	81.51 ± 1.91	SDSS DR12-BOSS
0.51	$D_M(r_{s,\text{fid}}/r_s)$	1977.4 ± 26.5	SDSS DR12-BOSS
0.51	$H(z)(r_s/r_{s,\text{fid}})$	90.45 ± 1.94	SDSS DR12-BOSS
0.61	$D_M(r_{s,\text{fid}}/r_s)$	2283.2 ± 31.9	SDSS DR12-BOSS
0.61	$H(z)(r_s/r_{s,\text{fid}})$	97.26 ± 2.09	SDSS DR12-BOSS
1.52	D_V/r_s	26.005 ± 0.995	SDSS DR14[38]

where we take the weak-scale cross section $\langle \sigma_w v \rangle \sim 10^{-26} \text{ cm}^3 \text{ s}^{-1}$ and T_b is the baryons temperature.

III. METHODS

We modify the public Boltzmann code CLASS [28, 29] to implement our model and to compute the theoretical values of the observables. Given the present-day Hubble parameter H_0 and the fraction of dark matter Ω_c , we can use the shooting method to obtain the initial conditions of ρ_c and ρ_d . Note that we only assume dark energy interacts with dark matter, so the evolution of baryons is unchanged. Then we use the code Monte Python [30, 31] which adopts the Markov chain Monte Carlo (MCMC) method to constrain the parameters in this model by fitting the cosmological data.

The data we have used includes CMB data, BAO data, redshift space distortion (RSD) data and SNe data. The CMB data consists of *Planck* 2015 temperature, polarization power spectrum (TT, TE, EE, low- ℓ) and lensing measurements [32, 33]. We also combine recent and reliable BAO and RSD measurements from various surveys, summarized in Tables I and II. As pointed out in Ref. [1], Quasar Ly α measurements are based on some assumptions and WiggleZ survey volume overlaps with BOSS-CMASS partly. So we do not include the BAO data from Quasar Ly α and WiggleZ in our analysis.

Table I shows the measurements of distance ratio D_V/r_s at the effective redshift. D_V is a combination of Hubble parameter $H(z)$ and comoving angular diameter distance $D_M(z)$ [1],

$$D_V(z) = \left[D_M^2(z) \frac{cz}{H(z)} \right]^{1/3}. \quad (21)$$

r_s is the comoving sound horizon at the end of the baryon drag epoch.

The peculiar velocity of galaxies could lead to distortion of clustering of galaxies in the redshift space. So measuring RSD effect can help us to probe the growth function. Table II shows the constraints on $f(z)\sigma_8(z)$

TABLE II: RSD measurements from various surveys adopted in this work.

Redshift	$f(z)\sigma_8(z)$	Surveys
0.02	0.428 ± 0.0465	Velocities from SNe [39]
0.067	0.423 ± 0.055	6dFGS [40]
0.15	0.49 ± 0.15	SDSS DR7-MGS [41]
0.3	0.49 ± 0.09	SDSS DR7-LRG [42]
0.18	0.36 ± 0.09	GAMA [43]
0.38	0.44 ± 0.06	GAMA
0.38	0.4975 ± 0.0451	SDSS DR12-BOSS
0.51	0.4575 ± 0.0377	SDSS DR12-BOSS
0.61	0.4361 ± 0.0344	SDSS DR12-BOSS
0.44	0.435 ± 0.055	WiggleZ [44]
0.60	0.451 ± 0.042	WiggleZ
0.73	0.478 ± 0.038	WiggleZ
0.6	0.55 ± 0.12	VIPERS [45]
0.86	0.40 ± 0.11	VIPERS
1.4	0.482 ± 0.116	FastSound [46]
1.52	0.426 ± 0.077	SDSS DR14 [47]

from various surveys. The scale-independent growth function is defined as

$$f(z) = \frac{d \ln D}{d \ln a}, \quad D(a) = \frac{\delta(a)}{\delta(a_0)}. \quad (22)$$

We use the SNe data from the ‘‘Pantheon Sample’’, which consists of 1048 SNe with the redshift spanning $0.01 < z < 2.3$. This sample is a combination of SNe Ia from Pan-STARRS1 Medium Deep Survey, SNLS, and several low- z and Hubble Space Telescope samples [48].

Due to the divergency of perturbations when w approaches -1 , we constrain the models with $w < -1$ and $w > -1$ separately. And for generality, we choose a broad range for the dark matter mass m_c . The prior ranges are set as

$$\alpha > 0, \quad (23)$$

$$\beta > 0, \quad (24)$$

$$-2 < w < -1 \quad \text{or} \quad -1 < w < -0.5, \quad (25)$$

$$1 \text{ eV} < m_c < 10 \text{ TeV}. \quad (26)$$

IV. RESULTS AND DISCUSSIONS

Fig. 1 shows the confidence contours for the parameters in the models $w < -1$ and $w > -1$. Tables III,IV summarize the best-fit parameters and 1σ , 2σ bounds from the CMB data and CMB+BAO+RSD+SNe dataset. We find the constraints for the two models $w < -1$ and $w > -1$ differ from each other significantly.

For the model $w < -1$, $\lambda \in (-0.05, 0.21)$ at 95% confidence level, indicating the deviation from Λ CDM model cannot be too large. And $\alpha \in (0.03, 0.63)$, $\beta \in (0, 3.6)$, $w \in (-1.072, -1)$ at 95% confidence level imply that a non-zero value of α is preferred by the dataset. If we limit the power indices to integers or half-integers for physical reasons, then the preferred values are $\alpha = 0.5$ and

$\beta = 0, 0.5, 1$. The inclusion of large-scale structure (LSS) and SNe data improves the constraints of λ significantly but has little impact on the other parameters.

For the model $w > -1$, we do not show the confidence regions of λ , because it can be very large to several hundred and could not converge. The 2σ confidence regions for the other parameters are $\alpha \in (0, 0.32)$, $\beta \in (20, 43)$ and $w \in (-0.9957, -0.9835)$. Thus a non-zero and large value of β is preferred by the data. In addition, w obeys a nearly Gaussian distribution, peaking at -0.99 . In this model, the viable parameter space is reduced by about 50% after including the LSS and SNe data.

In the following part, we take the best-fitting models as examples to discuss the background, perturbations and thermodynamics evolutions in the existence of interaction. In both best-fitting models, λ is positive, suggesting dark energy is converted to dark matter. Fig. 2 shows the evolutions of densities for dark matter and dark energy, compared with the Λ CDM model. To quantify the contribution of interaction to the density evolution, we compare the interaction term with expansion term in Fig. 3. The contribution of interaction increases with cosmic time and reaches the maximum at redshift $z \sim 1$. In the $w < -1$ model, the density of dark matter is enhanced by several percentage from $z \sim 1$ to the present day and the density of dark energy at $z = 10^4$ is about 30% of the present day value.

In the $w > -1$ model, a large β is favoured. So the interaction term $a\gamma\rho_c^\alpha\rho_d^\beta = aH_0\rho_{\text{cr}}\lambda(\rho_c/\rho_{\text{cr}})^\alpha(\rho_d/\rho_{\text{cr}})^\beta$ is negligible compared to the expansion terms. The density evolution of dark matter is nearly identical with Λ CDM model and the density evolution of dark energy is dominated by the equation of state w . Because the contributions of the interaction term to the background and perturbations evolutions are small, varying λ has little impact on the observables. So the data is insensitive to the variation of λ , and a convergent constraint for this parameter cannot be obtained in this model.

The cosmological perturbations are shown in Fig. 4. We only plot the density perturbation of dark matter in the Λ CDM model, while the evolution in the interacting model could have several percent deviation. For the dark energy, the density perturbation which is several orders smaller than δ_c grows and then keeps stable since $z \sim 10^4$. In the Λ CDM model, one usually sets $\theta_c = 0$ in the synchronous gauge. In the interacting models, θ_c has a tiny value. However, for dark energy, θ_d is extremely large, even several orders larger than θ_b . We note that to calculate θ_c , the term $k^2 c_c^2 \delta_c$ is in the same order of $aH\theta_c$ and even dominates in the range $0 < z < 10^4$ and $0.01 \text{ Mpc}^{-1} < k < 1 \text{ Mpc}^{-1}$. So this term cannot be dropped. But θ_c is really small and hence different choices of m_c have little impact on the evolution of the universe. We plot the posterior distribution of m_c in Fig. 5 and the distribution is nearly flat within the range $1 \text{ keV} - 1 \text{ TeV}$. The temperature evolutions of dark matter are shown in Fig. 6. Dark matter cools nearly adiabatically until $z \sim 1$ and the temperature is enhanced due

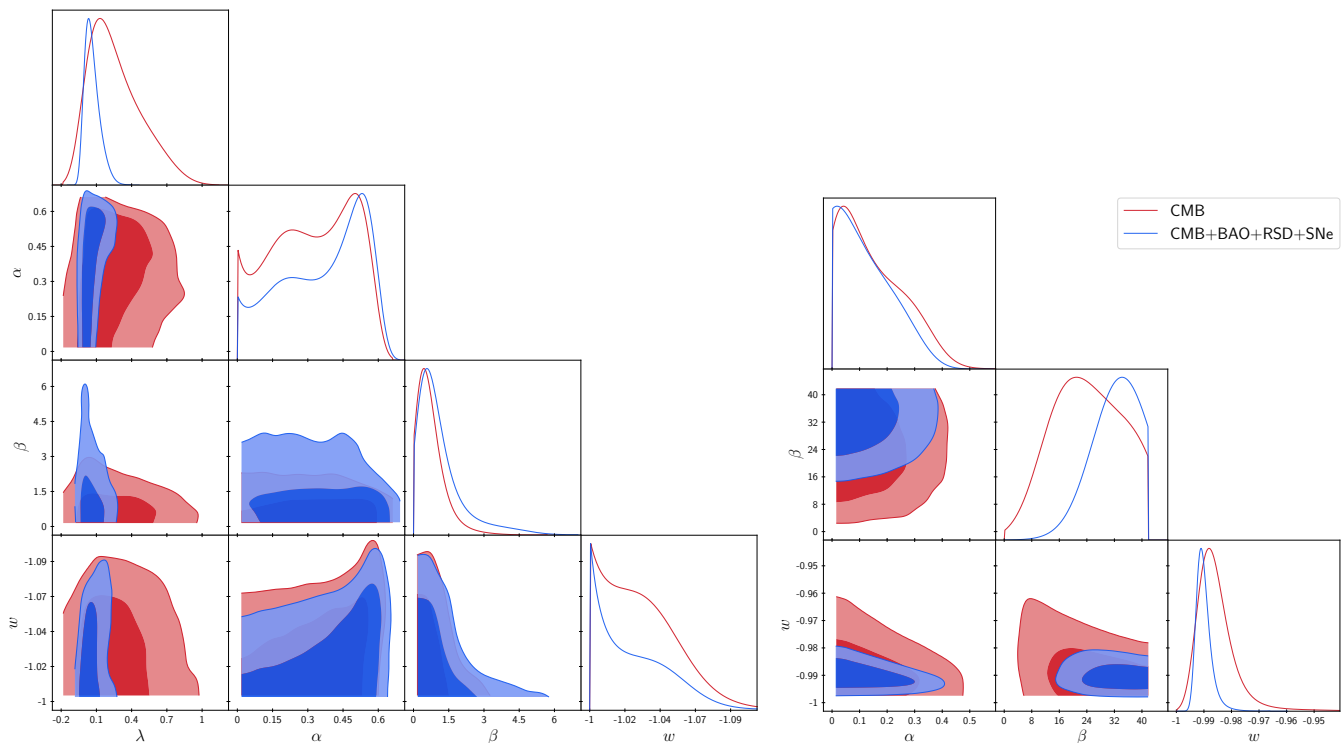


FIG. 1: One-dimensional marginalized posterior distribution and 68%, 95% confidence regions of the four free parameters in the model. The red lines correspond to the constraining results from CMB data only, and the blue lines correspond to joint constraints from CMB+BAO+RSD+SNe dataset. *Left* panel is for the model $w < -1$ and the *right* panel is for $w > -1$.

TABLE III: Constraints on the parameters in the model $w < -1$.

Parameter	<i>Planck</i> 68% C.L.	<i>Planck</i> 95% C.L.	<i>Planck</i> +BAO+RSD+SNe 68% C.L.	<i>Planck</i> +BAO+RSD+SNe 95% C.L.	<i>Planck</i> +BAO+RSD+SNe Best fit
λ	$0.27^{+0.15}_{-0.29}$	$0.27^{+0.47}_{-0.38}$	$0.060^{+0.031}_{-0.078}$	$0.06^{+0.15}_{-0.11}$	0.050
α	$0.32^{+0.24}_{-0.13}$	$0.32^{+0.26}_{-0.31}$	$0.37^{+0.25}_{-0.11}$	$0.37^{+0.26}_{-0.34}$	0.22
β	$0.80^{+0.19}_{-0.76}$	$0.80^{+1.3}_{-0.80}$	$1.19^{+0.11}_{-1.19}$	$1.2^{+2.4}_{-1.2}$	1.09
w	$-1.034^{+0.034}_{-0.011}$	$-1.034^{+0.034}_{-0.042}$	$-1.029^{+0.029}_{-0.010}$	$-1.029^{+0.029}_{-0.043}$	-1.047

TABLE IV: Constraints on the parameters in the model $w > -1$.

Parameter	<i>Planck</i> 68% C.L.	<i>Planck</i> 95% C.L.	<i>Planck</i> +BAO+RSD+SNe 68% C.L.	<i>Planck</i> +BAO+RSD+SNe 95% C.L.	<i>Planck</i> +BAO+RSD+SNe Best fit
α	$0.157^{+0.047}_{-0.16}$	$0.16^{+0.22}_{-0.16}$	$0.135^{+0.040}_{-0.13}$	$0.13^{+0.19}_{-0.13}$	0.031
β	24^{+11}_{-11}	24^{+19}_{-17}	$31.8^{+9.1}_{-4.7}$	32^{+11}_{-12}	34.6
w	$-0.9869^{+0.0028}_{-0.0083}$	$-0.987^{+0.016}_{-0.011}$	$-0.9901^{+0.0021}_{-0.0041}$	$-0.9901^{+0.0066}_{-0.0056}$	-0.9910

to the interaction by about 2% in the $w < -1$ model. According to Eq. (19), if $\gamma > 0$ dark matter is heated by dark energy and otherwise cooled.

The linear matter power spectrum at present is shown in Fig. 7. As illustrated in Fig. 4, the dark matter perturbations in the interacting model is similar with Λ CDM model. So the linear power spectrum makes little differ-

ence. The modification to the nonlinear power spectrum is much more significant and we will discuss it in the future paper.

We plot the evolutions of $f(z)\sigma_8(z)$ in our model and Λ CDM model in Fig. 8. $f\sigma_8 = a d\sigma_8(z)/da$ reveals the time derivative of matter fluctuations on the scale $8 h^{-1}\text{Mpc}$. Most measurements of $f(z)\sigma_8(z)$ at $z < 1$

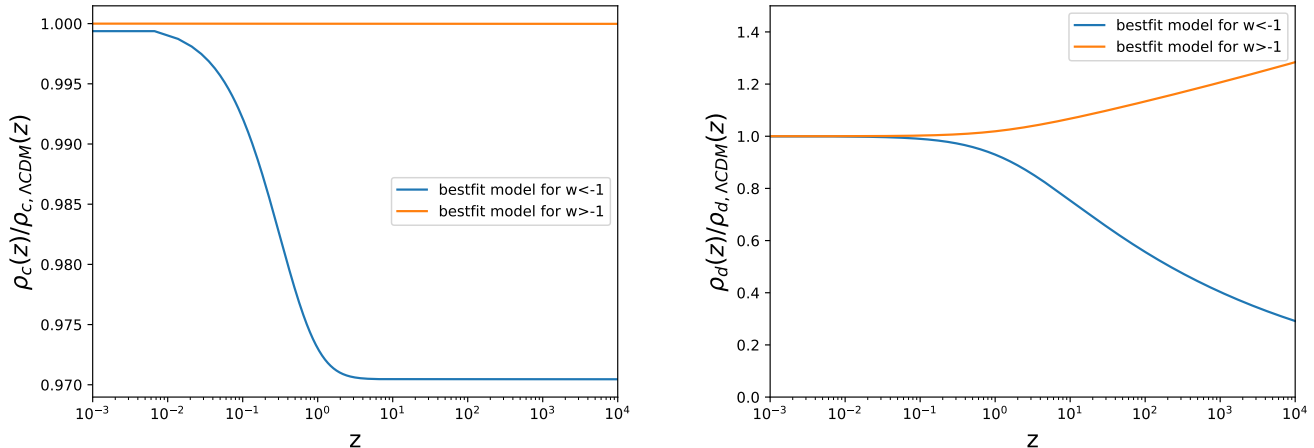


FIG. 2: The ratio of densities in the interacting models and Λ CDM model for dark matter (*left panel*) and dark energy (*right panel*) with respect to the redshift z . We choose the best-fitting models preferred by the CMB+BAO+RSD+SNe data set for the models $w < -1$ and $w > -1$.

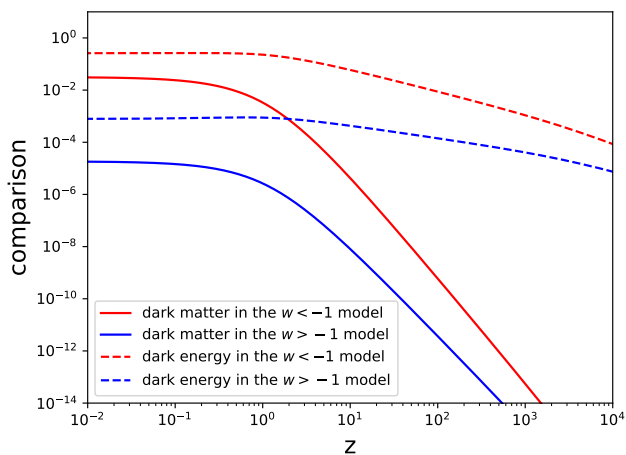


FIG. 3: The ratio of interaction term $a\gamma\rho_c^\alpha\rho_d^\beta$ and expansion term $3aH\rho_c$ for dark matter ($3a(1+w)H\rho_d$ for dark energy) in the same best-fitting models as Fig. 2.

are lower than that predicted by Λ CDM model. Coincidentally, as discussed above, the interaction mainly influences the late time evolution of the universe (roughly $z < 1$). In the $w < -1$ model, the evolution of $f(z)\sigma_8(z)$ is similar with Λ CDM model at high redshift and decreases since $z < 1$. So the fit to data points in our model is much better than the Λ CDM model, alleviating the tension at low redshift. Quantitatively, we calculate the reduced chi-square $\chi_\nu^2 = \chi^2/(n-m)$ to obtain the goodness of fit, where n is the number of data points and m is the number of free parameters. We fix the cosmological parameters in different models and hence there are 5 free parameters left. So χ_ν^2 is 0.56 for the $w < -1$ model and 0.75 for the Λ CDM model. Also, the curve predicted

by the $w < -1$ model is within all the 1σ bounds of the measurements used in this plot.

V. SUMMARY

In this paper, we consider the possible interaction between dark matter and dark energy and the impact on the evolution of universe. The interaction strength is proportional to some powers of the densities. We follow some previous work to derive the equations governing the evolutions of perturbations and thermodynamics in this model. And then we constrain the model using the latest cosmological data with the modified Boltzmann code.

For the $w > -1$ model, the data is insensitive to the variation of λ , and the 2σ bounds are $\alpha \in (0, 0.32)$, $\beta \in (20, 43)$, $w \in (-0.9957, -0.9835)$. A very large value of β is preferred by the data and w obeys the Gaussian distribution, peaking at -0.99 .

For the $w < -1$ model, the constraining results are $\lambda \in (-0.05, 0.21)$, $\alpha \in (0.03, 0.63)$, $\beta \in (0, 3.6)$ and $w \in (-1.072, -1)$ at 95% confidence level. While the non-interacting case ($\lambda = 0$) could accommodate the current data, a positive α is preferred, indicating the coupling strength between dark sectors may depend on ρ_c^α . For the physical reasons, one can choose the indices as integers or half-integers and the allowed values within 1σ regions are $\alpha = 0.5$ and $\beta = 0, 0.5, 1$. The inclusion of LSS and SNe data improves the constraints of some parameters significantly.

The background density evolution of dark matter could deviate from Λ CDM model by several percent. We also consider the perturbations in the existence of interaction and the impact on the structure formation and redshift space distortion. The density perturbation of dark matter could have deviation from Λ CDM model by several

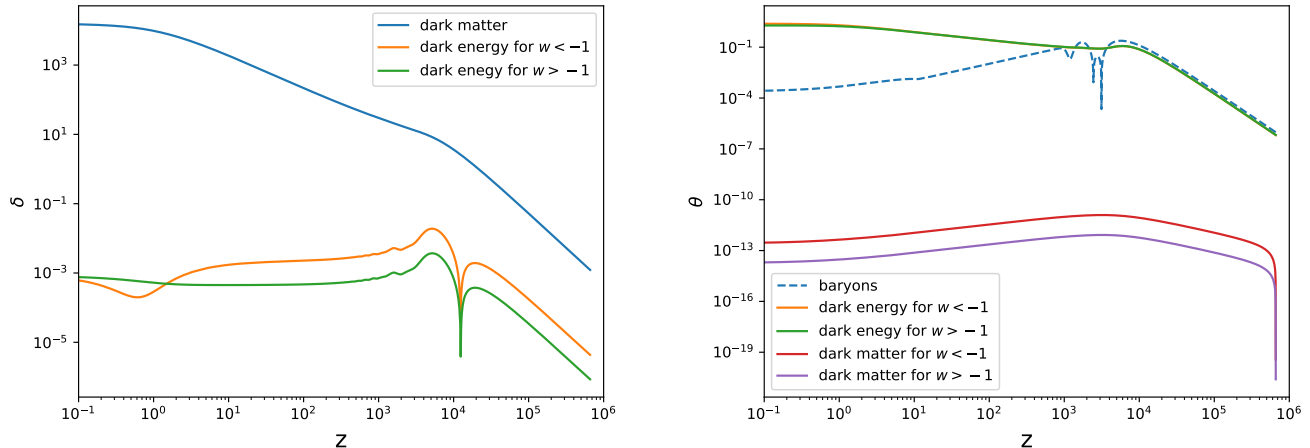


FIG. 4: The density (*left panel*) and velocity (*right panel*) perturbations for baryons, dark matter and dark energy on the scale $k = 0.1 \text{ Mpc}^{-1}$ in the same models as Fig. 2. The evolutions of δ_c are similar in different interacting models and Λ CDM model.

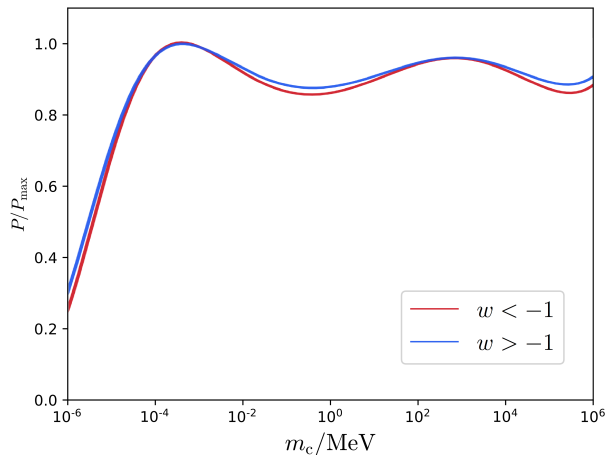


FIG. 5: One-dimensional marginalised probability distribution for the parameter m_c constrained by CMB+BAO+RSD+SNe dataset.

percent. Notably, θ_d is several orders larger than the velocity perturbation of baryons θ_b . We note that the term $k^2 c_c^2 \delta_c$ is dominant when calculating θ_c and hence could not be dropped. Because the velocity perturbation of dark matter is tiny, different choices of dark matter mass could hardly influence the results. In the $w < -1$

model, dark matter cools adiabatically, then heated due to the interaction by about 2% since $z \sim 1$.

The linear power spectrum in this model makes little difference and we will discuss the nonlinear power spectrum in the future paper. The observed $f(z)\sigma_8(z)$ values at $z < 1$ are mostly lower than that predicted by the Λ CDM model. As the effects of the interaction mainly appear at low redshift, the $w < -1$ model can alleviate the tension and fit the data points much better. Quantitatively, the reduced chi-square is 0.56 for the $w < -1$ model and 0.75 for the Λ CDM model. In summary, this class of interacting model in the phantom region ($w < -1$) is physically plausible and could provide better fit to the current CMB data from *Planck*, BAO and RSD data from SDSS and Type-Ia supernovae from Pantheon samples.

Acknowledgments

G.C., F. W. and X.C. acknowledge the support of the NSFC through grant No. 11633004, 11473044, U1501501, MoST through grant 2016YFE0100300, the CAS through QYZDJ-SSW-SLH017 and XDB 23040100. Y.Z.M. acknowledges the support of NRF with grant no.105925, 109577, and 120378, and NSFC with grant no. 11828301. J. Z. is supported by IBS under the project code, IBS-R018-D1.

-
- [1] Planck Collaboration, N. Aghanim, Y. Akrami, M. Ashdown, J. Aumont, C. Baccigalupi, M. Ballardini, A. J. Banday, R. B. Barreiro, N. Bartolo, et al., arXiv e-prints arXiv:1807.06209 (2018), 1807.06209.
 [2] L. Verde, T. Treu, and A. G. Riess, *Nature Astronomy*

- 3**, 891 (2019), 1907.10625.
 [3] G. Obied, H. Ooguri, L. Spodyneiko, and C. Vafa, arXiv e-prints arXiv:1806.08362 (2018), 1806.08362.
 [4] L. Santos, W. Zhao, E. G. M. Ferreira, and J. Quintin, *Phys. Rev. D* **96**, 103529 (2017), 1707.06827.

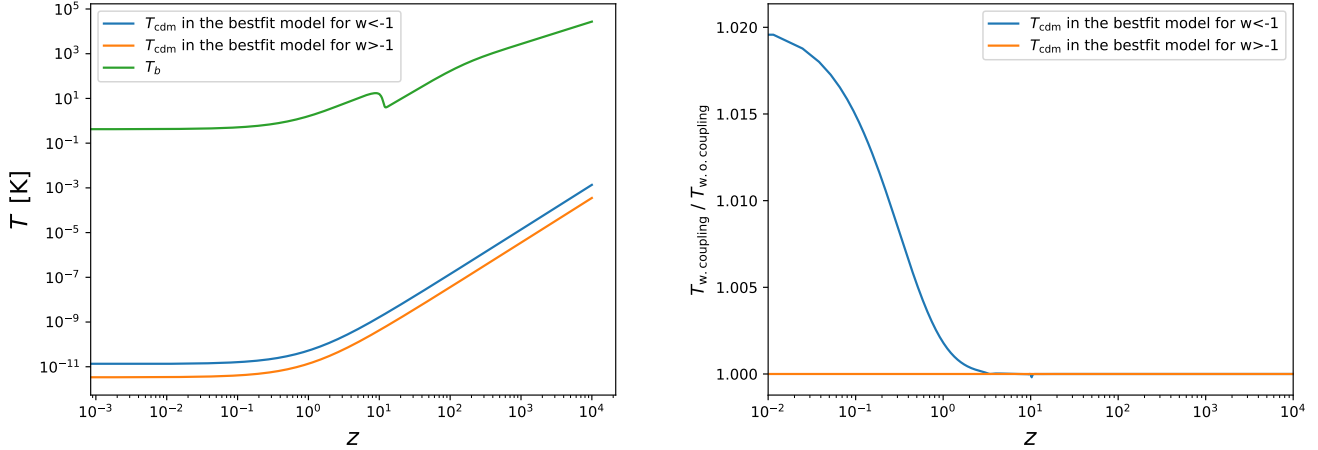


FIG. 6: *Left panel:* Temperature evolutions of baryons and dark matter in the best-fitting models as Fig. 2. *Right panel:* The ratio of temperature exactly evolved as Eq. (19) and the temperature in the case without coupling (cooling adiabatically) under the same initial condition.

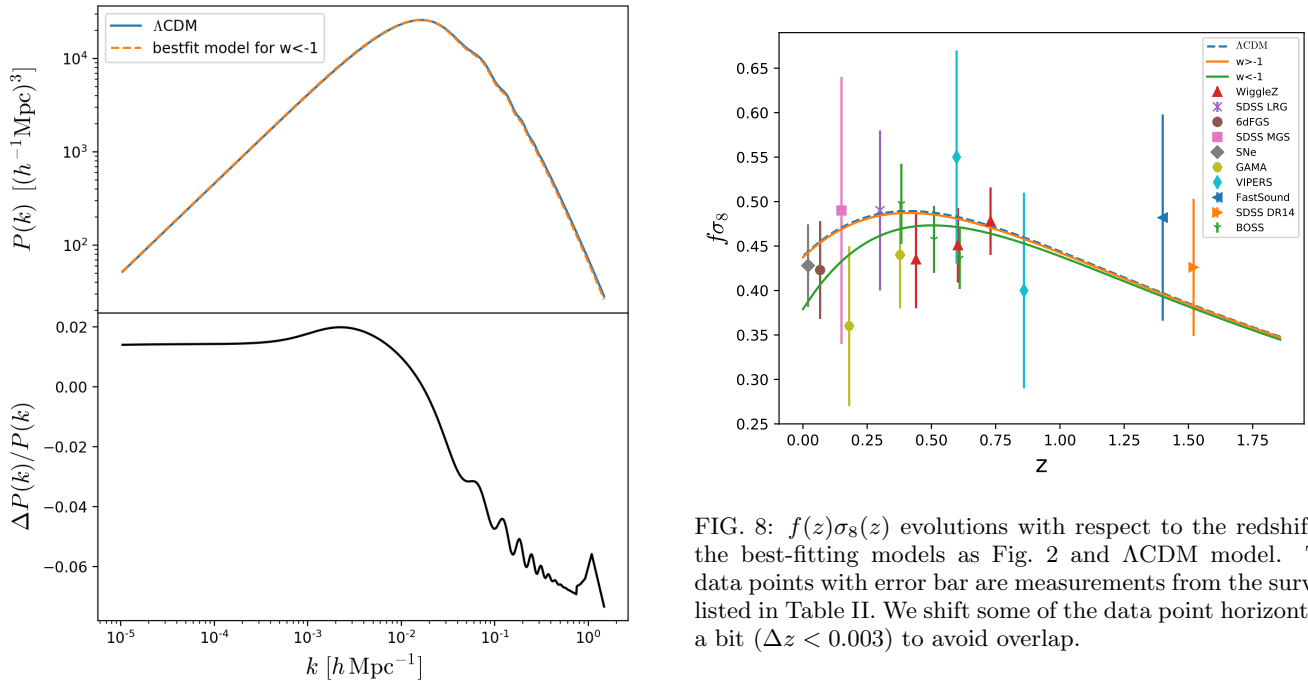


FIG. 7: *Top panel:* Linear matter power spectrum at $z = 0$ in the best-fitting models as Fig. 2. *Bottom panel:* The relative difference of matter power spectrum in the interacting model and Λ CDM model.

- [5] S. Kumar, R. C. Nunes, and S. K. Yadav, European Physical Journal C **79**, 576 (2019), 1903.04865.
 [6] E. Di Valentino, A. Melchiorri, O. Mena, and S. Vagnozzi, arXiv e-prints arXiv:1908.04281 (2019), 1908.04281.
 [7] A. A. Costa, X.-D. Xu, B. Wang, and E. Abdalla, JCAP **2017**, 028 (2017), 1605.04138.
 [8] C. van de Bruck and C. C. Thomas, Phys. Rev. D **100**,

023515 (2019), 1904.07082.

- [9] A. A. Costa, X.-D. Xu, B. Wang, E. G. M. Ferreira, and E. Abdalla, Phys. Rev. D **89**, 103531 (2014), 1311.7380.
 [10] B. Wang, E. Abdalla, F. Atrio-Barandela, and D. Pavón, Reports on Progress in Physics **79**, 096901 (2016), 1603.08299.
 [11] S. Wang, Y. Wang, and M. Li, Phys. Rep. **696**, 1 (2017), 1612.00345.
 [12] Y. L. Bolotin, A. Kostenko, O. A. Lemets, and D. A. Yerokhin, International Journal of Modern Physics D **24**, 1530007 (2015), 1310.0085.
 [13] M. Shahalam, S. D. Pathak, M. M. Verma, M. Y. Khlopov, and R. Myrzakulov, European Physical Journal

- C **75**, 395 (2015), 1503.08712.
- [14] S. del Campo, R. Herrera, and D. Pavón, *Phys. Rev. D* **91**, 123539 (2015), 1507.00187.
- [15] Y.-Z. Ma, Y. Gong, and X. Chen, *European Physical Journal C* **69**, 509 (2010), 0901.1215.
- [16] J. Mifsud and C. van de Bruck, *JCAP* **2017**, 001 (2017), 1707.07667.
- [17] G. Mangano, G. Miele, and V. Pettorino, *Modern Physics Letters A* **18**, 831 (2003), astro-ph/0212518.
- [18] M. B. Gavela, D. Hernández, L. Lopez Honorez, O. Mena, and S. Rigolin, *JCAP* **2009**, 034 (2009), 0901.1611.
- [19] L. Lopez Honorez, B. A. Reid, O. Mena, L. Verde, and R. Jimenez, *JCAP* **2010**, 029 (2010), 1006.0877.
- [20] M. B. Gavela, L. Lopez Honorez, O. Mena, and S. Rigolin, *JCAP* **2010**, 044 (2010), 1005.0295.
- [21] J.-H. He, B. Wang, and E. Abdalla, *Phys. Rev. D* **83**, 063515 (2011), 1012.3904.
- [22] C.-P. Ma and E. Bertschinger, *ApJ* **455**, 7 (1995), astro-ph/9506072.
- [23] J.-Q. Xia, Y.-F. Cai, T.-T. Qiu, G.-B. Zhao, and X. Zhang, *International Journal of Modern Physics D* **17**, 1229 (2008), astro-ph/0703202.
- [24] G. Ballesteros and J. Lesgourgues, *JCAP* **2010**, 014 (2010), 1004.5509.
- [25] R. Maartens, arXiv e-prints astro-ph/9609119 (1996), astro-ph/9609119.
- [26] V. H. Cárdenas, D. Grandón, and S. Lepe, *European Physical Journal C* **79**, 357 (2019), 1812.03540.
- [27] W. L. Xu, C. Dvorkin, and A. Chael, *Phys. Rev. D* **97**, 103530 (2018), 1802.06788.
- [28] J. Lesgourgues, arXiv e-prints arXiv:1104.2932 (2011), 1104.2932.
- [29] D. Blas, J. Lesgourgues, and T. Tram, *JCAP* **2011**, 034 (2011), 1104.2933.
- [30] B. Audren, J. Lesgourgues, K. Benabed, and S. Prunet, *JCAP* **2013**, 001 (2013), 1210.7183.
- [31] T. Brinckmann and J. Lesgourgues, arXiv e-prints arXiv:1804.07261 (2018), 1804.07261.
- [32] Planck Collaboration, R. Adam, P. A. R. Ade, N. Aghanim, Y. Akrami, M. I. R. Alves, F. Argüeso, M. Arnaud, F. Arroja, M. Ashdown, et al., *A&A* **594**, A1 (2016), 1502.01582.
- [33] Planck Collaboration, P. A. R. Ade, N. Aghanim, M. Arnaud, M. Ashdown, J. Aumont, C. Baccigalupi, A. J. Banday, R. B. Barreiro, J. G. Bartlett, et al., *A&A* **594**, A13 (2016), 1502.01589.
- [34] F. Beutler, C. Blake, M. Colless, D. H. Jones, L. Staveley-Smith, L. Campbell, Q. Parker, W. Saunders, and F. Watson, *MNRAS* **416**, 3017 (2011), 1106.3366.
- [35] A. J. Ross, L. Samushia, C. Howlett, W. J. Percival, A. Burden, and M. Manera, *MNRAS* **449**, 835 (2015), 1409.3242.
- [36] X. Xu, A. J. Cuesta, N. Padmanabhan, D. J. Eisenstein, and C. K. McBride, *MNRAS* **431**, 2834 (2013), 1206.6732.
- [37] S. Alam, M. Ata, S. Bailey, F. Beutler, D. Bizyaev, J. A. Blazek, A. S. Bolton, J. R. Brownstein, A. Burden, C.-H. Chuang, et al., *MNRAS* **470**, 2617 (2017), 1607.03155.
- [38] M. Ata, F. Baumgarten, J. Bautista, F. Beutler, D. Bizyaev, M. R. Blanton, J. A. Blazek, A. S. Bolton, J. Brinkmann, J. R. Brownstein, et al., *MNRAS* **473**, 4773 (2018), 1705.06373.
- [39] D. Huterer, D. L. Shafer, D. M. Scolnic, and F. Schmidt, *JCAP* **2017**, 015 (2017), 1611.09862.
- [40] F. Beutler, C. Blake, M. Colless, D. H. Jones, L. Staveley-Smith, G. B. Poole, L. Campbell, Q. Parker, W. Saunders, and F. Watson, *MNRAS* **423**, 3430 (2012), 1204.4725.
- [41] C. Howlett, A. J. Ross, L. Samushia, W. J. Percival, and M. Manera, *MNRAS* **449**, 848 (2015), 1409.3238.
- [42] A. Oka, S. Saito, T. Nishimichi, A. Taruya, and K. Yamamoto, *MNRAS* **439**, 2515 (2014), 1310.2820.
- [43] C. Blake, I. K. Baldry, J. Bland-Hawthorn, L. Christodoulou, M. Colless, C. Conselice, S. P. Driver, A. M. Hopkins, J. Liske, J. Loveday, et al., *MNRAS* **436**, 3089 (2013), 1309.5556.
- [44] C. Blake, S. Brough, M. Colless, C. Contreras, W. Couch, S. Croom, D. Croton, T. M. Davis, M. J. Drinkwater, K. Forster, et al., *MNRAS* **425**, 405 (2012), 1204.3674.
- [45] A. Pezzotta, S. de la Torre, J. Bel, B. R. Granett, L. Guzzo, J. A. Peacock, B. Garilli, M. Scodreggio, M. Bolzonella, U. Abbas, et al., *A&A* **604**, A33 (2017), 1612.05645.
- [46] T. Okumura, C. Hikage, T. Totani, M. Tonegawa, H. Okada, K. Glazebrook, C. Blake, P. G. Ferreira, S. More, A. Taruya, et al., *PASJ* **68**, 38 (2016), 1511.08083.
- [47] P. Zarrouk, E. Burtin, H. Gil-Marín, A. J. Ross, R. Tojeiro, I. Pâris, K. S. Dawson, A. D. Myers, W. J. Percival, C.-H. Chuang, et al., *MNRAS* **477**, 1639 (2018), 1801.03062.
- [48] D. M. Scolnic, D. O. Jones, A. Rest, Y. C. Pan, R. Chornock, R. J. Foley, M. E. Huber, R. Kessler, G. Narayan, A. G. Riess, et al., *ApJ* **859**, 101 (2018), 1710.00845.